

EVALUATION OF THE EFFECTS OF WEIGHT FRACTION ON THE AVERAGE CRYSTALLITE SIZE OF ZnO-SUPPORTED BIO-WASTE ACTIVATED CARBON COMPOSITES

*Onuoha David Chikaorama, Egbe Evudiovo Apha Peter, ¹Abdulrahman Asipita Salawu and ²Abdulkareem Ambali Saka

Mechanical Engineering Department,

¹Materials and Metallurgical Engineering Department,

²Chemical Engineering Department,

Federal University of Technology, P.M.B 65 Minna, Niger State, Nigeria.

*Corresponding author: onuoha.pg715804@st.futminna.edu.ng.

Abstract

Metal nanoparticles are known to possess outstanding mechanical properties, relative to their bulk materials. However, due to large surface energy, nanoparticles tend to coalesce to each other, forming bulk particles and eventually deteriorate in quality. It is therefore, essential to immobilize nanoparticles on a support to help particles stay away from each other. This paper reports the effects of weight fraction on the average crystallite size of ZnO supported groundnut shell based activated carbon composites. Preparation of activated carbon from groundnut shell was carried out by chemical activation process, using $ZnCl_2$ as activating agent at activation temperature, activation time and impregnation ratio of $600^\circ C$, 1.32 hrs and 3 respectively. Surface characterization was carried out on the prepared activated carbon to determine the surface morphology and proximate analysis of the sample. ZnO was synthesized using the sol-gel method with zinc acetate as precursor salt. The surface morphology and average particle size of synthesized ZnO were determined using scanning electron microscopy (SEM) and transmission electron microscope (TEM) respectively. Groundnut shell activated carbon (GSAC) and ZnO were mixed at different weight percentages (75:25, 50:50 and 25:75) to produce GSAC/ZnO composites. The composites developed were then characterized using X-ray diffraction (XRD). Relying on lattice parameters such as diffraction peaks and full width at half maximum (FWHM) obtained from the X-ray powder diffraction, the effects of weight fraction on the average crystallite size of ZnO supported GSAC composites were determined using Scherrer equation. The result obtained showed increase in average crystallite size with decrease in the amount of GSAC present in the GSAC/ZnO composite. The GSAC/ZnO composite with 75:25 weight fraction was found to have the smallest average crystallite size of 38.42 nm while GSAC/ZnO composite with 25:75 weight fraction was found to have the largest average crystallite size of 74.42 nm. The results suggest that the stabilization influence of groundnut shell activated carbon on ZnO reduced with increase in the amount of ZnO in the composites.

Keywords: Groundnut Shell, Activated Carbon, X-Ray Diffraction, Crystallite Size, Debye-Scherrer Method

1.0. INTRODUCTION

Given that activated carbon possesses extraordinary adsorption property and has for over two decades been predominantly used in treatment of wastewater, separation of gases and removal of heavy metals from industrial effluent, researchers are beginning to explore other areas of possible application for it. One of the new areas is in its use as support or host matrix for metal nanoparticles which is done with the intention of providing repulsive forces for prevention of coagulation of two metallic nanoparticles. Dispersion of metallic nanoparticles on solid supports such as activated carbon is essential in stabilization of metallic particles for spatial confinement of the particles in a nano range (Harish *et al.*, 2018). By taking into consideration the complex

interplay between matrix interface and nanoparticles, a good design of metal nanoparticles supported composite could tailor the composite material system into desirable physical properties (Hanemann and Szabo, 2010). Several underlying mechanisms are responsible for the interface reinforcement of the two phases. These mechanisms include the interaction between nanoparticles and the matrix which could result in the formation of special microstructures such as finer scale lamellar structure. Correspondingly, the outstanding mechanical properties associated with supported metal nanoparticles could prevent rapid crack propagation in a coating system (Burris, 2007).

Preparation methods of metal nanoparticles supported activated carbon are aimed at tailoring the

surface area chemistry of activated carbon to moderate the spatial behaviour of metal nanoparticles. This requires effective deposition of metal nanoparticles on the surface of a support, thereby enhancing dispersion and increasing the thermal stability of the metal nanoparticles. The interface between the nanoparticle and the matrix can be modified precisely on the molecular/atomic level with techniques such as atomic layer deposition (ALD) or molecular assembly to obtain some interesting structures as in the case of core/shell hybrid nanoparticles (Guo *et al.*, 2014). Supported metal oxide catalysts are commonly prepared by post synthesis methods such as impregnation or ion-exchange, co-precipitation and deposition precipitation (Serena, 2019).

Notably, formulation of metal nanoparticles supported bio-waste activated carbon composites is not only informed by the quest for development of engineering materials with improved targeted mechanical and functional properties, but also for cost effectiveness and environmental concerns. Renewability, environmental concerns and high cost of commercial activated carbons (activated carbons sourced from coal, petroleum residues, peat and lignite) are the major reasons for use of alternative sources of the material (Malik *et al.*, 2006; Yahya *et al.*, 2015). Therefore, this investigation has explored the preparation of activated carbon from most cost effective and environmentally friendly organic source using $ZnCl_2$ as activating agent in a chemical activation process. The common feature of all chemical activation process is the use of dehydrating agents which influence pyrolytic decomposition process and inhibit the formation of tar, thus enhancing the yield of activated carbon (Mansooreh and Tahereh, 2007). Typical advantage of using chemical activation include the possibility of achieving higher final carbon yield, the fact that it can be a one step process and the generally lower activation temperature involved when compared with physical activation process (Varila *et al.*, 2017). $ZnCl_2$ and H_3PO_4 are the commonly used activating agents for chemical activation of lignocelluloses materials (Williams and Reed 2004). However, $ZnCl_2$ could produce higher surface area as compared to H_3PO_4 (Al-Qoda and Shawabkah, 2009).

The sol-gel method used for production of ZnO has emerged as the simplest preparation technique for synthesizing metal nanoparticles (Azlina *et al.*, 2016). Unlike the more conventional methods, the sol-gel technique allows for preparation of materials in a 'one stop' with homogeneous distribution of components on atomic scale through a technology of low temperature synthesis and with full control

of the final product microstructure (Serena, 2019). The sol gel process involves the transition of a solution system from a liquid (sol) which is mostly colloidal into a solid (gel) phase (Sajjadi, 2005). The formation of metal oxide from sol- gel method involves different consecutive steps, first of which is the rapid hydrolysis of the corresponding metal precursor to produce the metal hydroxide solution, followed by immediate condensation which leads to the formation of three-dimensional gels, after which the resulting product is finally dried (Bolla *et al.*, 2017).

Generally desired properties such as improved toughness, increased hardness and enhanced corrosion resistance of nano-structured systems are strongly crystallite size and grain size dependent (Yin *et al.*, 2019; Muralidhara *et al.*, 2011). Smaller crystallite sizes result in drastic reduction in the required diffusing path for ions, thereby, enhancing system sorption kinetics significantly (Gubicza, 2017). It is therefore, necessary to examine the effects of weight fraction on the average crystallite size of ZnO supported groundnut shell activated carbon composites using one of the widely used tools (Scherrer equation) as results obtained may be vital for their engineering applications. X-ray diffraction (XRD) has been suggested as a convenient and well-known tool for calculating the average crystallite sizes in nanocrystalline and polycrystalline samples (Monshi *et al.*, 2012; Francisco *et al.*, 2016). Scherrer Equation was developed in 1918 to calculate nanocrystallite size by XRD radiation of wavelength λ (nm) from measuring full width at half maximum of peaks (β) in radians situated at any 2θ in the pattern (Monshi *et al.*, 2012). (Irfan *et al.*, 2018) gave the Scherrer formular for calculating the average crystallite size, D is as presented in Equation 1:

$$D = \frac{K\lambda}{\beta \cos\theta} \quad (1)$$

where D is the average crystallite size (nm), K is the shape factor ($K = 0.94$), λ is the x-ray wavelength in nanometer (nm), β is the full width at half maximum (FWHM) in radians and K is a constant related to crystallite shape, normally taken as 0.9. θ which is the expanded diffraction peak measured at full width at half maximum (FWHM) is in radians.

Scherrer equation is based on the assumption that each atom (scattering centre) scatters the incoming radiation independently, and once scattered the radiation does not interact with the other atoms. The derivation of the equation does not depend on the type of atoms inside the crystals, the structure factor of the reflection or the linear absorption coefficient (Francisco *et al.*, 2016).

2.0 MATERIALS AND METHODS

2.1 Materials

The chemicals and reagents used in the investigation were purchased from Joe Chem Ventures, Nsukka, Enugu state, Nigeria. The chemicals and reagents used in the synthesis of ZnO and formulation of GSAC/ZnO composites include zinc acetate dehydrate ($\text{Zn}(\text{CH}_3\text{COO})_2 \cdot 2\text{H}_2\text{O}$), isopropyl alcohol, distilled water, 2 M sodium hydroxide (NaOH), 1 M hydrochloric acid (HCl), ZnCl_2 (pellets) and acetone. All chemicals and reagents used are of analytical grade with percentage purity in the range of 95, - 99.6% and no further purifications were done.

Groundnut shells were purchased from groundnut sellers in Paiko market located in Minna, Niger State, Nigeria.

Other equipment used include LABE 1210 model muffle furnace, VEGA 3 TESCAN model scanning electron microscopy (SEM), EVO LS 10 model scanning electron microscopy, ZIESS EM900 transmission electron microscopy (TEM), magnetic stirrer, Siemens D-500 X-ray diffractometer (XRD), MicroActive ASAP 2460 volumetric adsorption analyzer and Equinox 55 FTIR spectrometer.

2.2 Methodology

2.2.1 Preparation of groundnut shell activated carbon (GSAC)

The groundnut shell was washed under tap water, sun-dried for two (2) weeks, crushed and sieved for particle size analysis. The dried particles that passed through the 48 μm sieve were loaded into a stainless steel vertical tubular reactor and put in a furnace for carbonization procedure. The temperature of the furnace was increased gradually from room temperature to 200°C under nitrogen (99.99%) flow at the flow rate of 150 ml/min. This temperature was kept constant for 3 hours to produce char. The char so produced was used for chemical activation. In carrying out chemical activation of groundnut char, a known weight (20 g) of the carbonized sample was mixed with ZnCl_2 pellets and dissolved in 250 ml of de-ionized water at impregnation ratio (IR) of 3 (Onuoha et al., 2019). The activation procedure was carried out in a muffle furnace with the temperature of the furnace raised to 600°C for 1.32 hrs (Onuoha et al., 2019). The impregnation ratio was determined using Equation 2.

$$\text{Impregnation ratio (IR)} = \frac{W_{\text{ZnCl}_2}}{W_{\text{char}}} \quad (2)$$

W_f of the sample retrieved from the furnace after activation as stated in Equation 3.

$$Y(\%) = \frac{W_f}{W_i} \times 100 \quad (3)$$

where $Y(\%)$ is the percentage yield, W_f is the final weight of activated sample and W_i is the initial weight of precursor before activation.

2.2.2 Characterization of GSAC

The prepared activated carbon was however, analysed for its moisture and ash content using the ASTM D 4442-92 and ASTM D 1102-84 methods respectively. The specific surface area of the sample was determined using BET isothermal equation. The total pore volume was estimated to be the liquid volume of nitrogen at a relative pressure of 0.98.

SEM was employed for examining the morphology of the prepared GSAC. Prior to SEM examination, the specimens were sputter-coated with gold to avoid charge accumulation. The FT-IR spectra of the sample were recorded by using the Equinox 55 FTIR spectrometer instrument. The spectra were recorded at room temperature with the wave number range of 4000 – 250 cm^{-1} . The N_2 adsorption isotherm was obtained by using the MicroActive ASAP 2460 volumetric adsorption analyser.

2.2.3 Synthesis of ZnO

The sol-gel method was used to synthesize ZnO. 100 ml of isopropyl alcohol was added to 15ml of zinc acetate dehydrate ($\text{Zn}(\text{CH}_3\text{COO})_2 \cdot 2\text{H}_2\text{O}$) and the mixture stirred vigorously for 10 minutes. 10 ml de-ionized water and 2M sodium hydroxide (NaOH) were added drop-wise to the solution and the mixture stirred continually for 2 hours to form a white gel which was left for 24 hours to dry. The dried ZnO was calcinated at 400°C to achieve the needed result. The sample was characterized using transmission electron microscopy (TEM) for particle size and scanning electron microscopy fitted with energy dispersive X-ray spectroscopy (SEM-EDS) for surface morphology and elemental composition.

2.2.4 Formulation of GSAC/ZnO composites

Three (3) composites (A, B and C) with varying weight percentage compositions of GSAC and ZnO (A: 75 wt.% of GSAC and 25 wt.% of ZnO; B: 50 wt.% of GSAC and 50 wt.% of ZnO; C: 25 wt.% of GSAC and 75 wt.% of ZnO) were formulated (Vineetha et al., 2018). To prepare the composites, each set of combination mixture was dissolved in 50 ml acetone and stirred vigorously using a magnetic stirrer at 30rev/min for 25 minutes to achieve homogeneity and even distribution of the constituents. The slurry formed was heated in an oven at 60°C for 4 hours to eliminate acetone (Lusi et al., 2017). XRD analysis of the different mixture ratios were carried out and their average crystallite sizes (D) calculated using the Debye Scherrer equation given in Equation 1.

3.0 RESULTS AND DISCUSSION

3.1 Characterization of GSAC

The result of the proximate analysis of GSAC is as presented in Table 1. The ash content was within the acceptable range of ≤ 8 max (ASTM). The low ash content of biomass resources make them good as a starting material for preparing activated carbon (Stavropoulos and Zabaniotou, 2005). The BET surface area for GSAC was observed to be above the $400 \text{ m}^2/\text{g}$ mark, which is the internal surface area value that generally defines activated carbons (McDougall 1991).

Table 1: Proximate Analysis Result for GSAC

S/N	Property	Value
1	pH	6.5
2	Moisture content (%)	2.5
3	Ash content (%)	7.5
4	Carbon yield (%)	50.02
5	BET average surface area (m^2/g)	498.52

The SEM micrograph of GSAC is as shown in Figure 1 revealing a heterogeneous surface with a variety of well-developed and randomly distributed pores. The randomly distributed pores observed on GSAC SEM image may have resulted from the activity of the activating agent (ZnCl_2) which, coupled with high activation temperature, may have dehydrated volatile constituents of the activated carbon structure, leaving empty spaces behind (Mohd *et al.*, 2015; Ioannidou and Zabaniotou, 2006).

Figure 2 shows the FTIR spectra of the prepared GSAC and the prevalent functional groups in the sample. The spectra revealed functional groups typical of any cellulosic material. Peaks at approximately 1582 cm^{-1} were observed for the GSAC sample indicating the C=O stretching vibration of lactone and carbonyl groups (Deng *et al.*, 2010). The GSAC exhibited hydroxyl functional groups, including O-H stretching with wave number range of about 3300 to 3500 cm^{-1} . The intense band at approximately 2920 cm^{-1} is assigned to asymmetric C-H stretching (Hesas *et al.*, 2013).

3.2 Characterization of ZnO nanoparticles

The scanning electron spectroscopy- energy dispersive spectroscopy (SEM-EDS) analysis of ZnO was carried out and the result presented in Figure 3. The SEM-EDS elemental composition of ZnO presented in Table 2 confirmed 63.98% and 36.02% presence of Zn and oxygen respectively. The SEM micrograph of prepared ZnO in Figure 3(a)

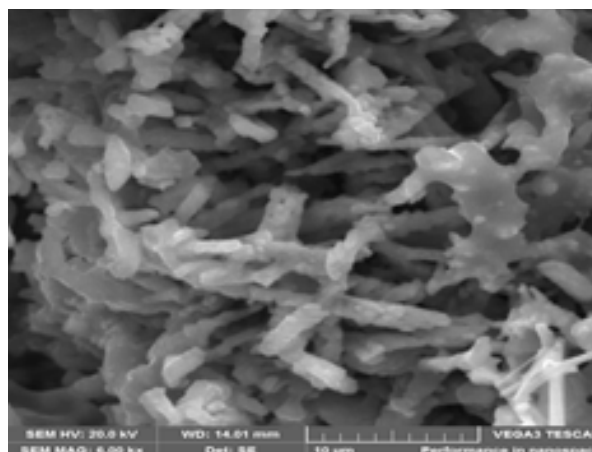


Figure 1: SEM image for GSAC

showed the morphologies of pure, predominantly regularly shaped and smooth ZnO particles with fine nanograins sizes. The absence of dots and coloured patches on the image indicated the absence of impurities. The SEM-EDS spectrum in Figure 3 (b) confirmed the presence of Zn at peaks of about 1.01, 8.62 and 9.50 keV.

The TEM micrograph for synthesized ZnO is as presented in Figure 4. Fine and well distributed rod shape of ZnO nanoparticles of average particle size of 12.0 to 14.0 nm were revealed in the ZnO

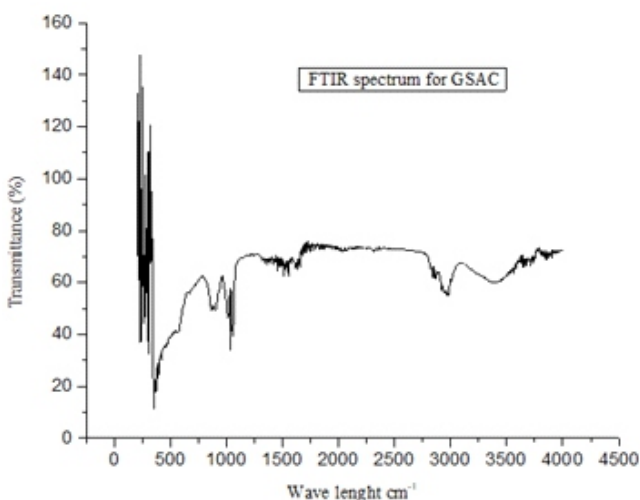
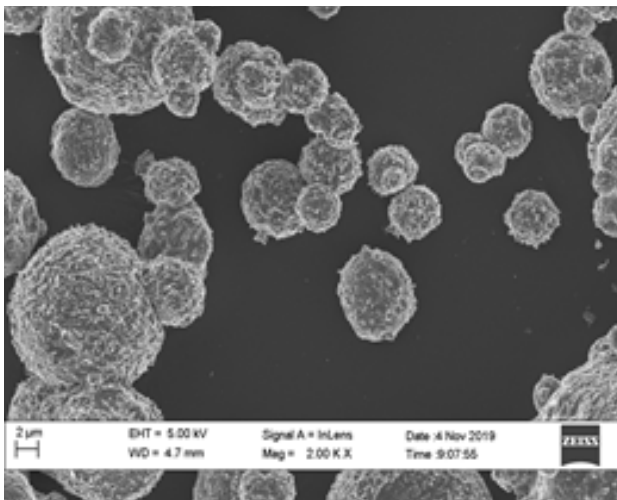


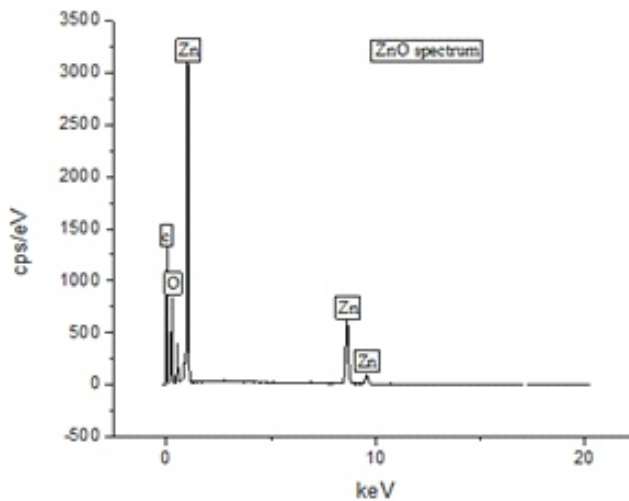
Figure 2: FTIR spectrum for GSAC

Table 2: SEM-EDS Elemental Composition of ZnO Nanoparticles

Element	wt. %
O	36.02
Zn	63.98
Total:	100



(a)



(b)

Figure 3: (a) SEM micrograph for ZnO and (b) EDS spectrum

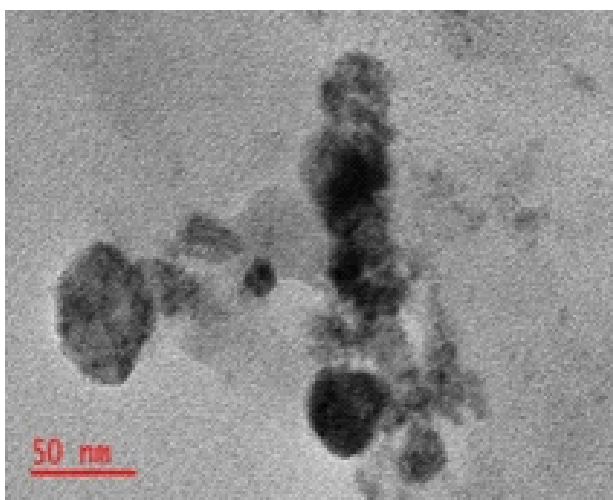


Figure 4: TEM micrograph for ZnO

TEM micrograph. A few particle aggregates were however, observed at some points. This could probably be because of the high surface energy associated with metal nanoparticles which make them agglomerate and deteriorate in quality (Harish *et al.*, 2018)..

3.3. X-Ray Diffractograph (XRD) Analysis of the Composites

The XRD spectra of the tested samples are as shown in Figure 5. The general sharp peaks exhibited by the three ZnO supported GSAC peaks composites could be related to the crystallinity of the samples (Irfan *et al.*, 2018). It was also observed that the number of major peaks formed increased with decreasing amount of the solid support offered by GSAC from composite A to C. It implies that there was increasing phase transformation as the amount of GSAC in the composites decreased. The increased phase transformation could be attributed to the weakening stabilization influence of the GSAC in the composite with increased amount of ZnO. With increased amount of ZnO in the composite, the restrictions offered by the GSAC are gradually overcome by ZnO, therefore, forming more compounds with elements associated with the inorganic activated carbon.

3.4 Determination of Average Crystal Size

Table 3 shows the calculated average crystallite size of the three different GSAC/ZnO composites (A:75 wt.% of GSAC and 25 wt % of ZnO); (B:50 wt.% of GSAC and 50 wt.% of ZnO) and (C:25 wt.% of GSAC and 75 wt.% of ZnO) The result of the calculated average crystallite size for GSAC/ZnO composites showed that average crystallite size increased from 38.42 nm to 74.42 nm as the weight composition of ZnO in the composites increased. The order of the average crystallite size of the composites being: Composite A < Composite B < Composite C. As the amount of ZnO in the composites increased from 25 wt. % in composite A to 50 wt.% in composite B and 75 wt.% in composite C, it is expected that the number of demobilized zinc ions would increase, thereby promoting thermal instability and improving the chances of ZnO nanoparticles embracing the thermodynamically favoured bulk particle state.

4.0 CONCLUSION

ZnO, which was synthesized using the Sol-gel method, was successfully hosted on the prepared groundnut shell activated carbon (GSAC) matrix at three different weight percentages to give three different composites. The average crystallites sizes

of the composites determined using Debye-Scherrer equation, demonstrated that GSAC is a good stabilization agent for ZnO. Composite A with the highest weight percentage composition of GSAC, gave the smallest average crystallite size of 38.42 nm, suggesting that with greater amount of GSAC present in the composites, GSAC tended to effectively moderate the spatial behaviour of ZnO by preventing ZnO ions from coalescing to each other to give bulk particles, thereby deteriorating in quality.

REFERENCES

- Al-Qodah, Z. Shawabkah, R., and Eliseo A. G., (2009). Production and Characterization of Granular Activated Carbon from Activated Sludge, *Braz J. Chem Eng*, 26(1): 127-36.
- Azlina, H. N., Hassidawani, J. N., Norita, H. and Surip, S. N. (2016) Synthesis of SiO₂ Nanostructure Using Sol- Gel Method, *ACTA Physica Polonica A* 129(4): 842-844
- Bolla, G. R., Debosshee, M. and Benjaram, M. R. (2017). Nanostructures for Novel Therapy: Synthesis, Characterization and Applications, A Volume in Micro and Nano Technologies Ed. Denisa, F. and Alexandru M. G. pp 1-36
- Burris, D. L. (2007) Effects of Nanoparticles on the Wear Resistance of Polytetrafluoroethylene Doctoral Thesis University of Florida, U. S. A.
- Deng, H., Zhang, G., Xu, X., Tao, G. and Dai, J. (2010). Optimization of Preparation of Activated Carbon from Cotton Stalk by Microwave Assisted Phosphoric Acid- Chemical Activation. *Journal of Hazardous Materials* 182, 217-224
- Francisco, T. L. M., Marcus, A. R. M., Cassio, M. dos Santos and Jose, M. S. (2016) The Scherrer Equation and Dynamical Theory of X-Ray Diffraction. *ACTA Crystallographica Section A: Foundations and Advances* 72 (3):385-390
- Gubicza J. (2017). Relationship between Microstructure and Hydrogen Storage Properties of Nanomaterials. Defect Structure and Properties of Nanomaterials 2nd and Extended Edition, 297 – 315.
- Guo, D., Xe, G. and Luo, J. (2014). Mechanical Properties of Nanoparticles: Basics and Applications. *J. Phys. D: Appl. Phys.* 47 (1):1-26.
- Hanemann T and Szabo D. V. (2010). Polymer - Nanoparticle Composites: From Synthesis to Modern Applications. *Materials* 3(6) 3468 – 3517.
- Harish, K. K., Nagasamy, V., Himangshu, B. and Anuttam, K. (2018). Metallic Nanoparticles: A Review. *Biomed J. Sci and Tech Res.* 4(2):3765-3775.
- Hesas, R. H., Arami-Niya, A., Daud, W. M. A.W. and Shahu, J. N. (2013). Preparation and Characterization of Activated Carbon from Apple Waste by Microwave-Assisted Phosphoric Acid Activation: Application in Methylene Blue Adsorption. *BioResources* 8(2) 2950-2966.
- Irfan, H., Mohamed, R. K. and Anand, S. (2018). Microstructural Evaluation of CoAl₂O₄ Nanoparticles by Williamson-Hall and Size-Strain Plot Method. *Journal of Asian Ceramic Societies* 6(1):54-62.
- Ioannidou, O. and Zabaniotou, A. (2006) Agricultural Residues as Precursors for Activated Carbon Production. *Renewable and Sustainable Energy Reviews* 11: 1966-2005.
- Lusi, E., Ratna, B., Takashi, O., Kikuo, O. and Tomonori, T. (2017). Role of Acetone in the Formation of Highly Dispersed Cationic Polystyrene Nanoparticles, *Chemical and Process Engineering*, 38(1), 5-18.
- Malik, R., Ramteke, D. S. and Wate, S. R. (2006). Physico- Chemical and Surface Characterization of Adsorbent Prepared from Groundnut Shell by ZnCl₂ Activation and its Ability to Adsorb Colour, *Indian Journal of Chemical Technology*, 13(4):319-328.
- Mansoorh, S. and Tahereh, K. (2007). Agricultural Waste Conversion to Activated Carbon by Chemical Activation with Phosphoric Acid, *Chemical Engineering Technology Journal*, 30(5): 649-654.
- McDougall, G. J. (1991). The Physical Nature and Manufacture of Activated Carbon, *Journal of the South African Institute of Mining and Metallurgy*, 91(4): 109-120.
- Mohd Adib Yahyaa, Z. Al-Qodah, n, C.W. Zanariah Ngaha (2015) Agricultural bio-waste materials as potential sustainable precursors used for activated carbon production: A review. *Renewable and Sustainable Energy Reviews* 46: 218-235
- Monshi, A., Foroughi, R. M. and Monshi, M. R. (2012). Modified Scherrer Equation to Estimate More Accurately Nanocrystallite Size Using XRD. *World Journal of Nano Science and Engineering*, 2(3):154-160.
- Muralidhara, H. B., Balasubramanyam, J., Arthobanaik, Y., Yogesh Kumar, K., Hanumanthappa, H. and Veena, M. S. (2011). Electrodeposition of Nanocrystalline Zinc on Steel Substrate from Acid Sulphate Bath and its Corrosion Study, *Journal of Chemical and Pharmaceutical Research*, 3(6): 433-449.
- Onuoha, D. C., Egbe, E. A. P., Abdulrahman, A. S. and Abdulkareem, A. S. (2019) Optimization of Process Variables in Bio-Waste Based Activated Carbon Preparation Using Response Surface Methodology. Book of Proceedings, 3rd International Engineering Conference (IEC 2019), Federal University of Technology, Minna, Nigeria, 581-589.
- Sajjadi, S. P. (2005). Sol-gel Process and its Application. *Journal of Polymer Engineering and Technology*, 13: 38-41
- Serena, E. (2019). Traditional Sol-Gel Chemistry as a Powerful Tool for the Preparation of Supported Metal and Metal Oxide Catalyst. *Materials*, 12: 668
- Stavropoulos, G. G. and Zabaniotou, A. A. (2005).

- Production and Characterization of Activated Carbons from Olive Seed Waste Residue. *Micropor Mesopor Mater*; 82: 79-85
- Varila, T., Bergna, D., Lahti, R., Romar, H., Hu, T. and Lassi, U. (2017). Activated Carbon from Peat Using ZnCl₂: Characterization and Applications. *BioResources* 12(4):8078-8092
- Vineetha, M., Shiyao, S., Chuan-Jian, Z. and Oana, MM. (2018). Effects of Chemical Composition on the Nanoscale Ordering Transformations of Physical Mixtures of Pd and Cu Nanoparticles. *Journal of Nanomaterials*, Article ID 9087320, 10.
- Williams, P. T and Reed, A. R. (2004). High Grade Activated Carbon Matting Derived from the Chemical Activation and Pyrolysis of Natural Fibre Textile Waste. *J Anal Appl Pyrol* 71:971-86.
- Yahya, M. A., Al-Qodahb, Z. and Zanariah Ngaha, C. W. (2015). Agricultural bio-waste materials as potential sustainable precursors used for activated carbon production: A Review. *Renewable and Sustainable Energy Reviews*, 46: 218-235.
- Yin, S., Chen, C. and Lupoi, R. (2019). Advanced Nanomaterials and Coatings by Thermal Spray. *Micro and Nano Spray* 27 -60.